PHYSICAL REVIEW A VOLUME 23, NUMBER 2 FEBRUARY 1981

Dynamic scattering function of liquid lead at 623 K

O. Söderström
Department of Reactor Physics, The Royal Institute of Technology, S-10044 Stockholm, Sweden
(Received 23 January 1980)

Liquid lead has been studied at 623 K by thermal neutron scattering technique. The range of momentum transfers is from 1.0 to 6.8 $Å^{-1}$. Up to 2.6 $Å^{-1}$ the highest energy transfer is 12 meV and above 2.6 $Å^{-1}$ it is 18 meV. The measurement is corrected for experimental effects including multiple scattering. No deconvolution of the resolution function has been performed. Normalization to the structure factor, obtained from an independent diffraction measurement has been done. The result is presented in the form of constant momentum transfers. The first and second moments have been compared with theoretical values. Intersections of the dynamic scattering function for constant momentum transfers between 1.0 and 1.4 $Å^{-1}$ show inelastic peaks originating from collective excitations in the liquid.

I. INTRODUCTION

In neutron scattering measurements the neutron applies a perturbation to the interacting particles in the sample. By measuring the changes of the neutron energy and momentum the dynamic scattering function can be determined. For a liquid it contains valuable information about the dynamical structure. If the scattering substance has an incoherent cross section, the dynamics of the self-motion of a particle can be studied. For a coherent scatterer, collective behavior can be revealed. During the last several years, the interest has been focused on performing coherent scattering measurements in the region of small Q values (Q is the momentum transfer), where inelastic peaks are expected to be seen. These peaks emanate from collective excitations created by density fluctuations. However, only a complete study for both small and large Q values can give relevant information about the dynamic structure completely. The dynamic properties of monatomic classical liquids have extensively been studied earlier by neutron scattering technique.[1,2]

A suitable substance for a neutron scattering study shall be totally coherent or incoherent. For technical reasons the melting point ought to be low. The velocity of sound shall be low so that the interesting part of the kinematic region can be reached by ordinary neutron sources and reasonably small observation angles.

Liquid argon is a classical liquid. By studying different mixtures of isotopes it was possible for Sköld *et al.*[3] to measure both the coherent and incoherent scattering functions. Liquid neon has a coherent cross section but is not a completely classical liquid. Its scattering function has been measured by Bell *et al.*[4] Another classical liquid with a coherent cross section is liquid rubidium. It has been studied by Copley and Rowe.[5] In argon no inelastic peaks could be seen in the observed Q range at atmospheric pressure, but in neon such peaks persisted up to 7% of Q_0 (Q_0 is the Q value of the first peak in the structure factor) and in rubidium up to 70% of Q_0.

The interaction between the atoms in a liquid is determined by the pair potential. In argon the potential is very near a Lennard-Jones potential, but in an alkali liquid metal the potential is completely different. The steep repulsive part is softer and around the minimum it is more harmonic. At large distances there are Friedel oscillations around zero due to the influence of the electrons. Unfortunately, the potential cannot be measured directly. Only indirect determinations are available. New methods have been developed, where the potential is calculated from the structure factor.[6,7] The result is very sensitive to the values and the shape of the measured structure factor at small Q values.[8] Such types of measurements are very complicated to perform and reliable potentials are difficult to obtain. Very recent molecular dynamics calculations in aluminum[9] have shown that essentially different potentials give very similar structure factors. However, there are indications that the repulsive part of the potential is different for monovalent and polyvalent metals. The valence and the electron structure also affect the potential in general.

As the potentials are very different for argon and rubidium, it is not surprising that collective excitations have been experimentally seen in rubidium but not in argon. Is rubidium a unique exception? It is an alkali metal, which is mostly monovalent. The atomic number is low (37) implying a fairly simple electron structure. To answer the question it is necessary to study a polyvalent metal with a high atomic number, which also means a large mass. The physical properties of two such metals are expected to be quite

different.

Lead is a good candidate for a neutron scattering experiment in order to answer the question above. It is polyvalent and the atomic number is large (82) and the mass is 207.21. The cross section is nearly totally coherent ($\sigma^c_{\text{bound}} = 11.31$ b) with a very small incoherent contamination ($\sigma^i_{\text{bound}} = 0.001$ b).[10] The absorption cross section is also very low ($\sigma^{\text{abs}} \simeq 0.1$ b at 1 Å). The melting point is 600 K and the velocity of sound, measured by ultrasonic methods, is 1.77×10^5 cm/s at 623 K.[11] A neutron of this velocity has a kinetic energy of 16.4 meV.

The first neutron scattering experiments were reported by Egelstaff[12] and Brockhouse.[13] Somewhat later Brockhouse and Pope[14] made a new measurement, where the multiple-scattering problem was treated. The second moment of the scattering function, the intermediate scattering function $F(Q,t)$, and the correlation function $G(r,t)$ were all evaluated from experimental values. Without doubt this was a pioneer work, where several significant aspects of a neutron scattering experiment were considered for the first time. Other experiments were performed by Pelah *et al.*,[15] Palevsky,[16] Turberfield,[17] and Cotter.[18] The measurement of Randolph and Singwi[19] was a continuation of the work of Brockhouse and Pope.[14] It was converted to constant Q values and normalized to the structure factor independently measured by neutron diffraction technique. The multiple scattering was considered later (Ref. 1, p. 503) and the first moment was evaluated. A table of their scattering function is presented in Table A2 of Ref. 1. The result was analyzed in the spirit of solidlike behavior. Cocking and Egelstaff[20,21] and Cocking[22,23] have measured liquid lead by cold neutrons. The result is presented in time-of-flight scale and a conversion to constant Q values was impossible to perform. Also Wignall and Egelstaff[24] used time-of-flight spectra for their analysis. Dorner, Plesser, and Stiller[25] measured at small constant Q values with a three axis spectrometer for thermal neutrons. The measurement was performed in a constant Q mode of operation. They found some inelastic peaks. The multiple scattering was, however, considerable and could not be determined and eliminated.

A very preliminary report of the present measurement, whose data sets have been reanalyzed here, has been published earlier.[26] However, the data analysis has been considerably improved and the region of observation extended. This measurement together with other new independent measurements[27] can report inelastic peaks up to about 60% of Q_0.

In Sec. II below some important formulas are given. The experimental details are briefly presented in Sec. III. In Sec. IV the data reduction procedures are described. The results with figures are presented in Sec. V and discussed in Sec. VI. Finally, some conclusions and outlooks are included in Sec. VII.

II. THEORY

Complete textbooks in the theory of thermal neutron scattering are Refs. 28 and 29. A time-of-flight experiment measures the double differential cross section for different angles and flight times. It can be transformed to the variables Q and E (E is the energy transfer). The double differential cross section is given by

$$\frac{d^2\sigma}{d\Omega\, dE} = \frac{\sigma_B^c}{4\pi}\left(\frac{E_0 - E}{E_0}\right)^{1/2} S(Q,E), \tag{1}$$

where Ω is the solid angle, σ_B^c the coherent bound-atom cross section, E_0 the incoming neutron energy, E the energy transferred to the scattering system, and $S(Q,E)$ the dynamic scattering function.

The symmetrized scattering function is defined by

$$\tilde{S}(Q,E) = e^{-E/2k_BT} S(Q,E), \tag{2}$$

where k_BT is the temperature in energy units. According to Schofield[30] the classical value of the scattering function can be approximated by its symmetrized form. The condition of detailed balance is then satisfied. Theoretical models of the scattering function are generally presented in classical form and a comparison can then directly be made with the experimental symmetrized scattering function.

The zeroth moment can be used for normalization to an independently measured structure factor. By calculating the first and second moments it is possible to check the quality of the obtained data sets. The intermediate scattering function $F(Q,t)$ measures density-density correlations and is given by

$$F(Q,t) = 2\int_0^\infty \cosh\left(\frac{E}{2k_BT} + i\frac{Et}{\hbar}\right)\tilde{S}(Q,E)\,dE \tag{3}$$

and is the Fourier transformation in space of the pair correlation function, $G(r,t)$.

Current-current correlations are measured by a quantity $C(Q,t)$ defined by

$$C(Q,t) = 2\int_0^\infty \cosh\left(\frac{E}{2k_BT} + i\frac{Et}{\hbar}\right)E^2\tilde{S}(Q,E)\,dE. \tag{4}$$

It is seen that $E^2\tilde{S}(Q,E)$ is a reasonable approx-

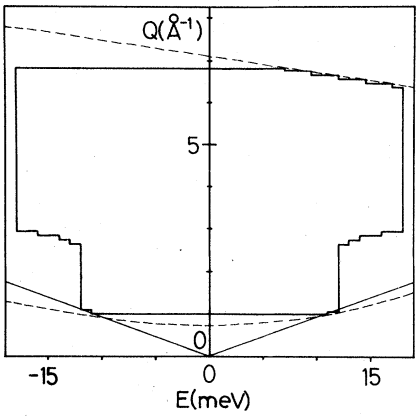

FIG. 1. The kinematic region covered by the two experiments (solid line). The dashed line at the small Q values shows the smallest observation angle for the lowest incoming energy and the one at large Q values the largest observation angle for the highest incoming energy. The velocity of sound, as measured by ultrasonic technique, is indicated.

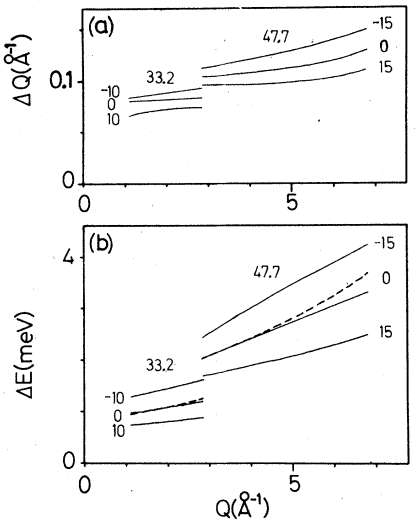

FIG. 2. (a) Momentum resolutions calculated for different energy transfers (in meV) at the two incoming energies (in meV). (b) Energy resolutions calculated for different energy transfers (in meV) at the two incoming energies (in meV) (full lines). The dotted lines are the elastic energy resolutions obtained from vanadium measurements.

imation of the spectral function. As Rahman[31] has shown, this spectral function has a maximum in E for constant Q. The position of the peak and the maximum value will change with Q.

The model of Ailawadi, Rahman, and Zwanzig[32] has been used for the multiple-scattering calculation. The model and its input parameters are presented in the Appendix.

III. EXPERIMENTAL DETAILS

The experiment was performed in the hybrid time-of-flight spectrometer for thermal neutrons at the material test reactor R2 in Studsvik. In Ref. 33 a detailed description of the instrument is found. Further details about the experiment are found in Ref. 26.

The kinematic region that was covered by the experiments is shown in Fig. 1. The total region available was cut when the intensity was too small to give reliable observations.

The energy and momentum resolutions were calculated[34] for different energy transfers with consideration taken to experimental effects. The results are shown in Figs. 2(a) and 2(b). The energy resolution for elastically scattered neutrons as obtained from vanadium measurements is shown in Fig. 2(b) and is also tabulated in Table I.

IV. DATA REDUCTION

Data program systems for data reduction in a time-of-flight experiment have been published earlier.[35] However, they are designed for a special experimental set-up and it is difficult to control their applicability to other experiments. For that reason a completely new program system has been developed. A full description is found in Ref. 36.

TABLE I. The energy resolution at elastic energy obtained from a vanadium measurement.

Q (Å^{-1})	ΔE (meV)	Q (Å^{-1})	ΔE (meV)	Q (Å^{-1})	ΔE (meV)
1.0	0.92	3.0	2.08	5.0	2.78
1.1	0.93	3.1	2.10	5.1	2.82
1.2	0.94	3.2	2.12	5.2	2.85
1.3	0.95	3.3	2.13	5.3	2.88
1.4	0.96	3.4	2.17	5.4	2.92
1.5	0.97	3.5	2.20	5.5	3.00
1.6	0.97	3.6	2.22	5.6	3.05
1.7	0.98	3.7	2.25	5.7	3.10
1.8	0.99	3.8	2.30	5.8	3.15
1.9	1.00	3.9	2.32	5.9	3.20
2.0	1.05	4.0	2.35	6.0	3.25
2.1	1.07	4.1	2.40	6.1	3.30
2.2	1.09	4.2	2.45	6.2	3.35
2.3	1.10	4.3	2.50	6.3	3.40
2.4	1.13	4.4	2.53	6.4	3.45
2.5	1.15	4.5	2.58	6.5	3.50
2.6	1.18	4.6	2.62	6.6	3.55
2.7	1.20	4.7	2.65	6.7	3.60
2.8	1.22	4.8	2.70	6.8	3.65
2.9	2.04	4.9	2.73		

A. Experimental effects

The first corrections of the raw data sets are described in Ref. 26. Some modifications have been made[36] as well as an attempt to estimate the errors.

B. Multiple scattering and self-shielding

There are two different methods to calculate the multiple-scattering contribution. The first method uses transport equations and only two scattering events can be calculated exactly.[37] The influences from higher-order scattering events can only be treated approximately and scattering from the surrounding container cannot be included. The effect of the resolution is also neglected. The second method uses the Monte Carlo technique and the whole experiment is simulated. All the disadvantages mentioned above are eliminated. A Monte Carlo program, especially developed by Copley[38] for time-of-flight experiments was used with the model of Ailawadi, Rahman, and Zwanzig[32] as input kernel. This model and its input parameters are fully explained in the Appendix. Also some remarks on the Monte Carlo program and a new subroutine have been used.[39] The number of neutrons was 3000. As has been pointed out by Copley and Lovesey in Ref. 1, pages 485–486, the ratio of single to multiple scattering is very sensitive to the model chosen and the instrumental resolution. The factor method was used in the earlier publication[26] but this method is inappropriate when the multiple scattering is large in comparison to the single-scattering contribution. A much better method is to calculate the multiple-scattering contribution and then subtract it from the normalized data sets. The direct influence of the model dependent first scattering event is then eliminated. The problem is that absolutely normalized data sets are needed. However, the experimental data sets can be renormalized and one possibility is suggested in Sec. IV C below. Even for this case the multiple scattering is dependent on the model, but the major contribution comes from large Q values, where the models are similar. However, to test the influence of the model chosen, a new, less extensive multiple-scattering calculation was performed with the model values replaced by the obtained experimental values in regions where they are available. As the experimental values contain the resolution, the model was folded with the resolution according to Table I and the Monte Carlo program was run with a perfect resolution. The simulation of the experiment was then not quite correct but it is a reasonable approximation.

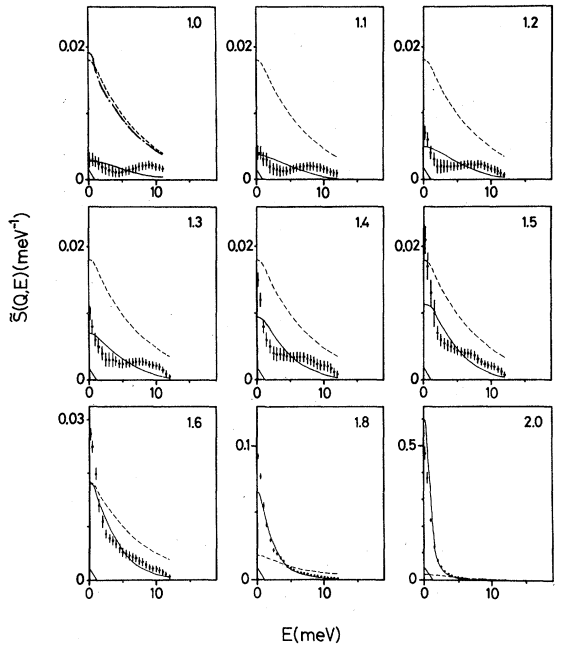

FIG. 3. The symmetrized scattering function for different Q values (in Å^{-1}) below Q_0. The dots with the error bars come from the experiments. The full line is the model, described in the Appendix, folded with the resolution in Table I. The dashed line is the mean value of the energy gain and energy loss data of the multiple scattering. The resolution is also indicated. At 1.0 Å^{-1} the dash-dotted line is from another multiple-scattering calculation described in the text.

The result is included in Fig. 3 and it is seen that the difference is fairly small. The multiple scattering was not calculated for all angles and energy transfers that were measured. Intermediate values were obtained by interpolation. The multiple scattering in vanadium was also taken into account. It was about 10%. The multiple-scattering values contain self-shielding. After the subtraction of the multiple-scattering contribution the remaining values, representing single scattering, could be corrected for self-shielding.

C. Normalization of data sets

In the preceding section it was pointed out that absolutely normalized data are necessary in order to allow subtraction of the multiple scattering. It has not been possible to get an absolute normalization of this experiment directly and, therefore, it has been necessary to apply a renormalization procedure. The multiple scattering varied very little with Q for a constant-E cut. So it could easily be interpolated to constant-Q values and integrated over E. The structure factor of the multiple-scattering contribution was then

TABLE II. Symmetrized scattering function for liquid lead at 623 K. The error is in the last significant figure.

E (meV) \ Q (Å^{-1})	1.0	1.1	1.2	1.3	1.4	1.5
0	0.003±1	0.004±1	0.007±1	0.010±1	0.015±1	0.021±2
0.5	0.003±1	0.004±1	0.006±1	0.008±1	0.012±1	0.017±2
1.0	0.0028±9	0.003±1	0.004±1	0.006±1	0.008±1	0.013±2
1.5	0.0025±9	0.003±1	0.003±1	0.005±1	0.006±1	0.010±2
2.0	0.0021±9	0.002±1	0.002±1	0.004±1	0.005±1	0.007±1
2.5	0.0018±9	0.0017±9	0.002±1	0.003±1	0.004±1	0.0059±9
3.0	0.0015±8	0.0015±9	0.0021±9	0.003±1	0.0038±9	0.0055±8
3.5	0.0013±8	0.0014±9	0.0020±9	0.003±1	0.0037±9	0.0053±8
4.0	0.0012±7	0.0014±7	0.0020±6	0.0028±7	0.0037±8	0.0050±7
4.5	0.0012±7	0.0014±7	0.0020±6	0.0026±6	0.0036±7	0.0046±7
5.0	0.0013±6	0.0015±6	0.0021±6	0.0026±6	0.0034±7	0.0043±7
5.5	0.0014±6	0.0016±6	0.0022±6	0.0026±6	0.0033±7	0.0041±6
6.0	0.0016±6	0.0017±6	0.0023±6	0.0026±6	0.0033±7	0.0040±6
6.5	0.0017±6	0.0018±6	0.0023±6	0.0027±6	0.0034±7	0.0040±6
7.0	0.0019±6	0.0020±6	0.0023±6	0.0027±6	0.0033±7	0.0039±6
7.5	0.0021±6	0.0021±6	0.0022±6	0.0027±6	0.0031±7	0.0036±6
8.0	0.0022±6	0.0021±6	0.0023±6	0.0027±6	0.0029±7	0.0032±6
8.5	0.0022±6	0.0021±6	0.0023±6	0.0024±5	0.0027±7	0.0027±5
9.0	0.0023±6	0.0021±5	0.0020±6	0.0022±5	0.0025±7	0.0023±5
9.5	0.0022±6	0.0019±5	0.0019±5	0.0022±5	0.0024±7	0.0023±5
10.0	0.0021±6	0.0018±5	0.0018±5	0.0022±5	0.0024±7	0.0022±5
10.5	0.0019±5	0.0015±5	0.0016±5	0.0018±5	0.0021±7	0.0022±5
11.0	0.0016±5	0.0013±5	0.0012±5	0.0013±5	0.0016±7	0.0016±5
11.5		0.0011±5	0.0009±5	0.0009±5	0.0011±6	0.0011±5
12.0		0.0010±5	0.0007±4	0.0007±4	0.0008±4	0.0008±4

obtained. It was seen, as a first approximation, that this structure factor was independent of Q. Its nature was "incoherent" as expected. It is denoted by M below. The original data sets were converted to constant Q according to the procedure described in the following Sec. IV D. No correction for multiple scattering was included. The structure factor was obtained by integration over E. It is denoted by $I(Q)$ below. The data sets were then renormalized by the following linear regression line:

$$\alpha I(Q) - \beta = S(Q), \tag{5}$$

where α is the slope, β the intercept, and $S(Q)$ the structure factor obtained from an independent diffraction measurement.[40,41] The intercept β is the structure factor of the multiple scattering and is compared to the calculated M by

$$\gamma = \beta/M. \tag{6}$$

The original multiple-scattering values, coming out from the Monte Carlo program, are given for different angles and energy transfers. They were multiplied by γ. The original experimental data sets were multiplied by α and then the corresponding scaled multiple-scattering contribution was subtracted. After that the interpolation to constant Q was made (see Sec. IV D below). The standard deviation in the multiple-scattering contribution was included in the total statistical error.

The first measurement was performed from 1.0 to 2.8 Å^{-1}. At Q values below about 1.8 Å^{-1} the multiple scattering dominated over the single scattering. Thus the most important term in the regression line (5) was the intercept β and, therefore, it could be carefully determined. At Q values greater than about 1.8 Å^{-1} the multiple scattering was comparatively small and the regression line was dominated by the term $\alpha I(Q)$. The slope α could be carefully obtained. Owing to this balancing feature of the Q region covered by this measurement, the linear regression line approach of renormalization could be justified.

The situation was different in the second experiment, which covered a range from 2.9 to 6.8 Å^{-1}. The multiple scattering here was comparatively small over the whole Q region and the intercept β in the linear regression line (5) could not be adequately determined. Hence the γ value

TABLE II. *(Continued)*

E (meV) \ Q (Å^{-1})	1.6	1.7	1.8	1.9	2.0	2.1
0	0.027 ± 1	0.047 ± 2	0.092 ± 2	0.188 ± 7	0.47 ± 2	0.99 ± 4
0.5	0.025 ± 1	0.042 ± 2	0.077 ± 2	0.164 ± 7	0.38 ± 2	0.78 ± 4
1.0	0.020 ± 1	0.032 ± 2	0.055 ± 2	0.114 ± 2	0.224 ± 3	0.399 ± 8
1.5	0.014 ± 1	0.023 ± 2	0.041 ± 1	0.074 ± 2	0.122 ± 2	0.179 ± 7
2.0	0.011 ± 1	0.017 ± 1	0.029 ± 1	0.050 ± 1	0.071 ± 2	0.093 ± 2
2.5	0.0086 ± 9	0.0141 ± 9	0.022 ± 1	0.035 ± 1	0.048 ± 1	0.060 ± 2
3.0	0.0078 ± 8	0.0123 ± 9	0.019 ± 1	0.026 ± 1	0.034 ± 1	0.041 ± 2
3.5	0.0075 ± 8	0.0109 ± 8	0.016 ± 1	0.021 ± 1	0.025 ± 1	0.028 ± 2
4.0	0.0069 ± 7	0.0093 ± 8	0.013 ± 1	0.0154 ± 9	0.018 ± 1	0.0195 ± 9
4.5	0.0060 ± 7	0.0079 ± 8	0.010 ± 1	0.0128 ± 9	0.014 ± 1	0.0139 ± 8
5.0	0.0053 ± 7	0.0073 ± 7	0.009 ± 1	0.0109 ± 9	0.0114 ± 7	0.0110 ± 8
5.5	0.0049 ± 7	0.0063 ± 7	0.007 ± 1	0.0071 ± 9	0.0069 ± 7	0.0092 ± 7
6.0	0.0047 ± 7	0.0052 ± 7	0.006 ± 1	0.0055 ± 7	0.0056 ± 7	0.0068 ± 7
6.5	0.0044 ± 6	0.0042 ± 7	0.0048 ± 9	0.0046 ± 6	0.0050 ± 7	0.0048 ± 7
7.0	0.0040 ± 6	0.0039 ± 6	0.0044 ± 8	0.0040 ± 6	0.0043 ± 7	0.0039 ± 6
7.5	0.0035 ± 6	0.0036 ± 6	0.0039 ± 6	0.0035 ± 6	0.0034 ± 7	0.0035 ± 6
8.0	0.0034 ± 6	0.0032 ± 6	0.0032 ± 5	0.0031 ± 5	0.0026 ± 7	0.0030 ± 6
8.5	0.0028 ± 5	0.0029 ± 5	0.0028 ± 5	0.0028 ± 5	0.0021 ± 7	0.0024 ± 6
9.0	0.0023 ± 5	0.0026 ± 5	0.0025 ± 5	0.0025 ± 5	0.0019 ± 7	0.0019 ± 5
9.5	0.0023 ± 5	0.0023 ± 5	0.0022 ± 5	0.0021 ± 5	0.0018 ± 7	0.0016 ± 5
10.0	0.0022 ± 5	0.0020 ± 5	0.0018 ± 5	0.0016 ± 5	0.0016 ± 7	0.0015 ± 5
10.5	0.0019 ± 5	0.0014 ± 5	0.0014 ± 5	0.0011 ± 5	0.0013 ± 6	0.0014 ± 5
11.0	0.0014 ± 4	0.0013 ± 5	0.0010 ± 4	0.0011 ± 4	0.0011 ± 6	0.0011 ± 4
11.5	0.0009 ± 4	0.0009 ± 5	0.0007 ± 4	0.0006 ± 4	0.0007 ± 4	0.0008 ± 4
12.0	0.0006 ± 4	0.0007 ± 5	0.0005 ± 4	0.0005 ± 4	0.0005 ± 4	0.0005 ± 3

in equation (6) was put equal to unity. A mean value of α was obtained from equation (5). The original experimental data sets were multiplied by α and the calculated multiple-scattering contribution was subtracted without being scaled.

The result of the renormalization was that for the first measurement the values $\alpha = 0.85$ and $\gamma = 1.15$ were obtained. The second experiment gave $\alpha = 0.91$.

By the procedures described above the experimental data sets were normalized to the structure factor and the result of the measurement is not absolutely normalized. The reason why a renormalization had to be performed is discussed in Sec. VI below.

D. Conversion to constant Q

After having subtracted the multiple-scattering contribution a cubic spline function[42] fit was applied for every energy transfer. The chosen energy step was 0.5 meV. As weight function the inverse of the absolute error was used. However, it was necessary to develop some control routines to avoid numerical instabilities which could create unsatisfying fluctuations in the results.[36] The scattering function was calculated in Q steps of 0.1 Å^{-1} which is about the Q resolution.

A new spline function fit was applied for every Q. The scattering function was calculated from Eq. (1) and the symmetrized scattering function from Eq. (2). Due to the experiment and the procedures involved in the data reduction, the energy scale was shifted slightly at each Q. To correct for that, the first moment of the symmetrized scattering function was minimized by changing the energy scale within the energy resolution. Then the first three moments were calculated.

As has been pointed out by Johnson *et al.*[43] the calculation of the errors is particularly difficult in these types of measurements. However, it is better to give a rough estimate of the errors than to give no errors at all. The statistical errors from the detectors were reduced when mean values within the energy step were taken. These errors were directly transformed to errors in the symmetrized scattering function. It is clear that the errors must be overestimated by this procedure, because the influence of the spline function fits was not taken into consideration.

In the final result the mean value of the scattering functions at positive and negative energy transfers was calculated. The statistical error was then reduced. If the asymmetry was larger than the reduced error value, it was chosen as

TABLE II. *(Continued)*

E (meV) \ Q (Å^{-1})	2.2	2.3	2.4	2.5	2.6	2.7
0	1.34 ± 1	1.03 ± 4	0.60 ± 3	0.38 ± 2	0.27 ± 1	0.213 ± 4
0.5	1.02 ± 1	0.81 ± 4	0.50 ± 3	0.33 ± 2	0.25 ± 1	0.187 ± 4
1.0	0.511 ± 6	0.44 ± 1	0.31 ± 2	0.23 ± 1	0.18 ± 1	0.142 ± 3
1.5	0.222 ± 3	0.209 ± 7	0.174 ± 6	0.14 ± 1	0.118 ± 7	0.100 ± 2
2.0	0.108 ± 2	0.110 ± 4	0.104 ± 2	0.091 ± 2	0.081 ± 5	0.071 ± 2
2.5	0.066 ± 2	0.067 ± 1	0.067 ± 1	0.063 ± 1	0.058 ± 2	0.052 ± 1
3.0	0.043 ± 1	0.044 ± 1	0.047 ± 1	0.046 ± 1	0.044 ± 1	0.040 ± 1
3.5	0.029 ± 1	0.033 ± 1	0.034 ± 1	0.036 ± 1	0.033 ± 1	0.031 ± 1
4.0	0.0220 ± 9	0.025 ± 1	0.025 ± 1	0.026 ± 1	0.027 ± 1	0.026 ± 1
4.5	0.0164 ± 8	0.0179 ± 9	0.0190 ± 8	0.0203 ± 9	0.0208 ± 9	0.0207 ± 9
5.0	0.0113 ± 7	0.0127 ± 8	0.0145 ± 8	0.0159 ± 9	0.0164 ± 9	0.0163 ± 9
5.5	0.0086 ± 7	0.0100 ± 8	0.0114 ± 8	0.0126 ± 8	0.0134 ± 9	0.0136 ± 9
6.0	0.0069 ± 6	0.0077 ± 7	0.0089 ± 8	0.0103 ± 8	0.0112 ± 9	0.0117 ± 9
6.5	0.0054 ± 6	0.0064 ± 7	0.0073 ± 8	0.0085 ± 8	0.0095 ± 9	0.0101 ± 9
7.0	0.0044 ± 6	0.0049 ± 6	0.0061 ± 8	0.0070 ± 8	0.0081 ± 9	0.0087 ± 9
7.5	0.0036 ± 5	0.0040 ± 6	0.0052 ± 8	0.0056 ± 8	0.0070 ± 9	0.0075 ± 9
8.0	0.0029 ± 5	0.0034 ± 5	0.0041 ± 6	0.0046 ± 6	0.0057 ± 9	0.0063 ± 9
8.5	0.0024 ± 5	0.0029 ± 5	0.0033 ± 6	0.0033 ± 6	0.0047 ± 7	0.0053 ± 9
9.0	0.0020 ± 5	0.0025 ± 5	0.0028 ± 6	0.0029 ± 6	0.0035 ± 7	0.0043 ± 9
9.5	0.0017 ± 5	0.0021 ± 5	0.0023 ± 5	0.0027 ± 6	0.0033 ± 7	0.0037 ± 9
10.0	0.0015 ± 4	0.0016 ± 5	0.0017 ± 5	0.0026 ± 5	0.0031 ± 7	0.0033 ± 9
10.5	0.0013 ± 4	0.0013 ± 5	0.0012 ± 5	0.0019 ± 5	0.0024 ± 6	0.0023 ± 9
11.0	0.0011 ± 4	0.0011 ± 4	0.0007 ± 4	0.0014 ± 5	0.0016 ± 5	0.0018 ± 7
11.5	0.0009 ± 4	0.0009 ± 4	0.0005 ± 4	0.0013 ± 5	0.0012 ± 5	0.0015 ± 5
12.0	0.0008 ± 4	0.0007 ± 4	0.0005 ± 4	0.0013 ± 5	0.0012 ± 5	0.0009 ± 5
12.5						0.0005 ± 4
13.0						0.0005 ± 4

the error. This means that both the energy gain and energy loss data sets were contained within the assigned error. Finally, the error bars were slightly modified so that they were decreasing in magnitude for increasing energy transfers at constant Q.

E. Resolution

No attempts were made to defold the resolution function because there are no reliable methods developed. However, the resolution affects the asymmetry of the symmetrized scattering function, but this was considered when the error was determined, i.e., the influence of the resolution was within the error bars. The resolution was assumed to be a Gaussian with the full width at half maximum (FWHM) according to Table I. Theoretical models shall be folded with the resolution before they can be compared with the experimental results.

V. RESULTS

The symmetrized dynamic scattering function is presented in Table II for selected Q and E values.[44] In Fig. 3 the table values are shown for some constant Q values below Q_0. The mean value of the energy gain and energy loss data for the calculated multiple-scattering contribution is also plotted into the figure to show its dominating effect, especially at the smallest Q values. Another multiple-scattering calculation is also shown at 1.0 Å^{-1} (see above). Scattering function at and above Q_0 is shown in Fig. 4 and here the multiple scattering does not dominate. Intersections of the scattering function at constant energy transfers are shown in Fig. 5 and the spectral function $E^2\bar{S}(Q, E)$, according to Eq. (4), in Fig. 6. The multiple scattering is also shown here to demonstrate its large influence particularly at high energy transfers. The zeroth moment was calculated and compared with the neutron diffraction results[40,41] in Fig. 7. The first and second moments were determined and compared with exact theoretical values as exposed in Fig. 8(a) and 8(b). The fact that they look similar depends upon the small value of $E/2k_BT$ which indeed confirms that liquid lead is a classical liquid.

TABLE II. *(Continued)*

E (meV) \ Q (Å^{-1})	2.8	3.0	3.2	3.4	3.7	4.1
0	0.159±4	0.088±9	0.085±9	0.109±5	0.163±4	0.187±4
0.5	0.144±4	0.084±9	0.081±9	0.105±5	0.157±4	0.181±4
1.0	0.111±4	0.074±9	0.073±9	0.092±5	0.138±4	0.163±4
1.5	0.082±4	0.062±9	0.062±9	0.076±5	0.113±4	0.141±4
2.0	0.061±4	0.051±6	0.050±8	0.060±4	0.091±3	0.118±4
2.5	0.046±3	0.041±4	0.040±6	0.047±3	0.072±3	0.097±3
3.0	0.036±2	0.034±2	0.033±4	0.039±3	0.057±2	0.079±2
3.5	0.030±1	0.028±2	0.027±3	0.032±1	0.046±1	0.065±1
4.0	0.025±1	0.023±1	0.023±2	0.027±1	0.0378±8	0.0530±8
4.5	0.0197±9	0.0199±8	0.021±1	0.024±1	0.0317±7	0.0434±8
5.0	0.0160±9	0.0170±7	0.018±1	0.0208±7	0.0272±7	0.0356±7
5.5	0.0140±9	0.0148±7	0.0164±9	0.0184±7	0.0235±6	0.0295±7
6.0	0.0119±9	0.0130±7	0.0147±9	0.0167±7	0.0203±6	0.0247±6
6.5	0.0104±9	0.0117±7	0.0133±9	0.0149±5	0.0174±5	0.0211±6
7.0	0.0092±9	0.0108±7	0.0120±9	0.0135±5	0.0146±5	0.0182±5
7.5	0.0081±9	0.0100±7	0.0109±9	0.0127±5	0.0129±5	0.0153±5
8.0	0.0071±9	0.0092±7	0.0098±8	0.0118±4	0.0112±5	0.0133±5
8.5	0.0061±9	0.0081±7	0.0086±5	0.0103±4	0.0103±4	0.0113±5
9.0	0.0056±9	0.0066±7	0.0080±5	0.0090±4	0.0093±4	0.0099±5
9.5	0.0048±9	0.0057±7	0.0070±5	0.0081±4	0.0082±4	0.0086±5
10.0	0.0039±9	0.0052±7	0.0060±5	0.0072±4	0.0071±4	0.0073±5
10.5	0.0036±9	0.0045±7	0.0052±5	0.0064±4	0.0062±4	0.0062±5
11.0	0.0029±9	0.0038±7	0.0044±5	0.0056±4	0.0054±4	0.0053±5
11.5	0.0025±7	0.0031±7	0.0038±5	0.0049±4	0.0048±4	0.0046±5
12.0	0.0014±5	0.0026±7	0.0033±5	0.0043±4	0.0044±4	0.0041±5
12.5	0.0012±5	0.0023±7	0.0030±5	0.0037±4	0.0039±4	0.0037±5
13.0	0.0011±5	0.0020±7	0.0027±5	0.0032±4	0.0030±3	0.0034±5
14.0	0.0006±4	0.0017±7	0.0021±5	0.0024±4	0.0025±3	0.0028±5
15.0		0.0015±7	0.0018±5	0.0019±4	0.0020±3	0.0021±3
16.0		0.0013±7	0.0016±5	0.0016±4	0.0017±2	0.0020±3
17.0		0.0011±7	0.0011±5	0.0014±4	0.0015±2	0.0015±3
18.0		0.0010±6	0.0009±3	0.0013±4	0.0015±2	0.0015±1

VI. DISCUSSION

The measurements were normalized to the structure factor by the procedures described in Sec. IV C above. There were two reasons why a renormalization procedure had to be preformed. Firstly, the electronics could not be kept exactly stable during these long measuring times. Secondly, the number of scattering atoms could not be completely determined. The thicknesses of the sample and the vanadium plate were difficult to control and measure with enough accuracy. The experimental values were not extrapolated to higher energy transfers. As can be seen in Figs. 3, 4, and 6 the integration over E will have truncation errors at the determination of the moments. However, the final zeroth moment gave satisfactory values over the whole Q range except around 6.1 Å^{-1}, where a peak in the structure factor coincided with a Bragg peak from the container (see Fig. 7). The first and second moments are sensitive to the resolution and the multiple-scattering correction. As the resolution was not defolded and the multiple scattering was considerable in some regions, these moments cannot be expected to be absolutely correct. Figure 8 shows that both the first and second moments are about 25% too high. No error bars are shown as systematic truncation errors, mentioned above, are included. The figure gives an idea of the quality of the measurement.

The renormalized data sets, corrected for multiple scattering, had clearly visible reminiscences of inelastic peaks at small Q values (Fig. 3). A "dispersion" relation can be constructed and is shown in Fig. 9 together with independently obtained results from experiments in a three axis spectrometer.[27] The velocity of sound is also indicated in the figure. The error bars are estimated uncertainties in the determina-

TABLE II. *(Continued)*

E (meV) \ Q (Å^{-1})	4.3	4.6	5.1	5.6	6.5	6.8
0	0.158 ± 2	0.107 ± 1	0.065 ± 1	0.083 ± 2	0.060 ± 2	0.051 ± 5
0.5	0.154 ± 2	0.105 ± 1	0.065 ± 1	0.082 ± 2	0.060 ± 2	0.051 ± 5
1.0	0.142 ± 2	0.099 ± 1	0.065 ± 1	0.079 ± 2	0.058 ± 2	0.051 ± 5
1.5	0.126 ± 2	0.091 ± 1	0.062 ± 1	0.075 ± 2	0.057 ± 2	0.050 ± 5
2.0	0.108 ± 2	0.080 ± 1	0.057 ± 1	0.069 ± 2	0.055 ± 2	0.049 ± 5
2.5	0.091 ± 2	0.070 ± 1	0.052 ± 1	0.063 ± 2	0.053 ± 2	0.047 ± 5
3.0	0.077 ± 2	0.061 ± 1	0.047 ± 1	0.057 ± 2	0.050 ± 2	0.045 ± 5
3.5	0.064 ± 1	0.054 ± 1	0.042 ± 1	0.052 ± 2	0.048 ± 2	0.043 ± 5
4.0	0.0538 ± 9	0.0479 ± 8	0.039 ± 1	0.047 ± 2	0.046 ± 1	0.041 ± 5
4.5	0.0461 ± 9	0.0423 ± 8	0.036 ± 1	0.042 ± 2	0.044 ± 1	0.039 ± 3
5.0	0.0375 ± 8	0.0365 ± 8	0.0330 ± 7	0.037 ± 2	0.041 ± 1	0.037 ± 2
5.5	0.0311 ± 7	0.0315 ± 7	0.0295 ± 7	0.033 ± 1	0.038 ± 1	0.0337 ± 9
6.0	0.0273 ± 6	0.0278 ± 7	0.0270 ± 6	0.030 ± 1	0.034 ± 1	0.0306 ± 7
6.5	0.0229 ± 6	0.0247 ± 7	0.0247 ± 6	0.026 ± 1	0.031 ± 1	0.0281 ± 7
7.0	0.0197 ± 5	0.0220 ± 7	0.0224 ± 6	0.024 ± 1	0.029 ± 1	0.0266 ± 7
7.5	0.0174 ± 5	0.0195 ± 7	0.0204 ± 5	0.021 ± 1	0.027 ± 1	0.0246 ± 7
8.0	0.0151 ± 5	0.0171 ± 7	0.0187 ± 5	0.019 ± 1	0.025 ± 1	0.0230 ± 7
8.5	0.0131 ± 4	0.0150 ± 7	0.0170 ± 5	0.017 ± 1	0.024 ± 1	0.0216 ± 7
9.0	0.0113 ± 4	0.0133 ± 7	0.0154 ± 5	0.015 ± 1	0.0206 ± 8	0.0204 ± 7
9.5	0.0096 ± 4	0.0112 ± 7	0.0138 ± 5	0.0137 ± 9	0.0188 ± 8	0.0193 ± 6
10.0	0.0082 ± 4	0.0102 ± 4	0.0124 ± 5	0.0123 ± 9	0.0171 ± 8	0.0181 ± 6
10.5	0.0071 ± 4	0.0090 ± 4	0.0111 ± 5	0.0109 ± 9	0.0154 ± 8	0.0165 ± 5
11.0	0.0061 ± 4	0.0078 ± 3	0.0099 ± 5	0.0097 ± 8	0.0137 ± 8	0.0149 ± 5
11.5	0.0053 ± 4	0.0068 ± 3	0.0088 ± 5	0.0085 ± 7	0.0124 ± 8	0.0133 ± 5
12.0	0.0047 ± 4	0.0058 ± 3	0.0078 ± 5	0.0074 ± 7	0.0111 ± 8	0.0119 ± 5
12.5	0.0041 ± 4	0.0050 ± 3	0.0066 ± 5	0.0069 ± 7	0.0097 ± 8	0.0107 ± 5
13.0	0.0037 ± 4	0.0044 ± 3	0.0058 ± 5	0.0061 ± 7	0.0085 ± 8	0.0097 ± 4
14.0	0.0028 ± 4	0.0033 ± 3	0.0045 ± 5	0.0047 ± 7	0.0074 ± 8	0.0084 ± 4
15.0	0.0021 ± 3	0.0027 ± 3	0.0036 ± 5	0.0037 ± 6	0.0057 ± 8	0.0070 ± 4
16.0	0.0018 ± 2	0.0024 ± 3	0.0025 ± 5	0.0030 ± 4	0.0042 ± 8	0.0049 ± 4
17.0	0.0016 ± 2	0.0015 ± 2	0.0025 ± 5	0.0024 ± 3	0.0036 ± 7	0.0044 ± 4
18.0	0.0014 ± 1	0.0014 ± 1	0.0015 ± 1	0.0018 ± 3	0.0026 ± 6	0.0035 ± 4

tion of the position of the inelastic peak. As can be seen in Fig. 9 all the three measurements coincide within the uncertainties. The reason why the peaks were observed in this time-of-flight measurement to higher Q values than in the three axis measurements is that the former was corrected for multiple scattering and the latter were not.

The FWHM for different Q values was determined and the resolution was quadratically subtracted. The result is shown in Fig. 10. The correction for resolution is correct only when the scattering function is a Gaussian, but it is a reasonable approximation. The error bars are the uncertainty in the determination of the widths. For an ideal gas the width w of the symmetrized scattering function is given by

$$w^{ig} = 2\left(\frac{2k_B T \ln 2}{M}\right)^{1/2} Q . \tag{7}$$

This straight line is shown in Fig. 10. The width of the scattering function for a diffusive process is given by

$$w^{\mathrm{diff}} = 2\hbar D Q^2 , \tag{8}$$

where D is the diffusion coefficient whose value is found in Ref. 45, page 164. The parabola is also shown in Fig. 10. The figure shows that liquid lead, as expected, even for the highest Q values is very far from a gas state. The experimental curve has its minima, where the structure factor has its maxima. This behavior is similar to what has been observed in other liquids.[3,5]

The spectral function $E^2\tilde{S}(Q, E)$ used in Eq. (4) has a maximum in energy at a constant Q value (see Fig. 6). The position of the peak, $E_{\max}$, is plotted against the corresponding Q value in Fig. 11. The $E_{\max}$ value for an ideal gas is given by

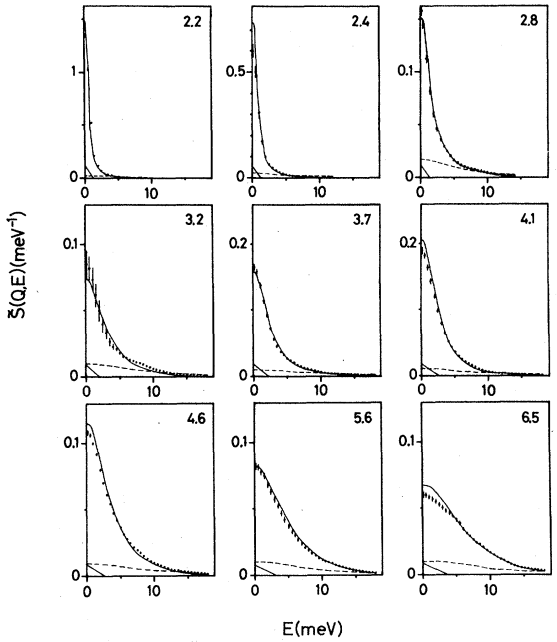

FIG. 4. The symmetrized scattering function for different Q values (in Å^{-1}) at and above Q_0. The notations are the same as in Fig. 3.

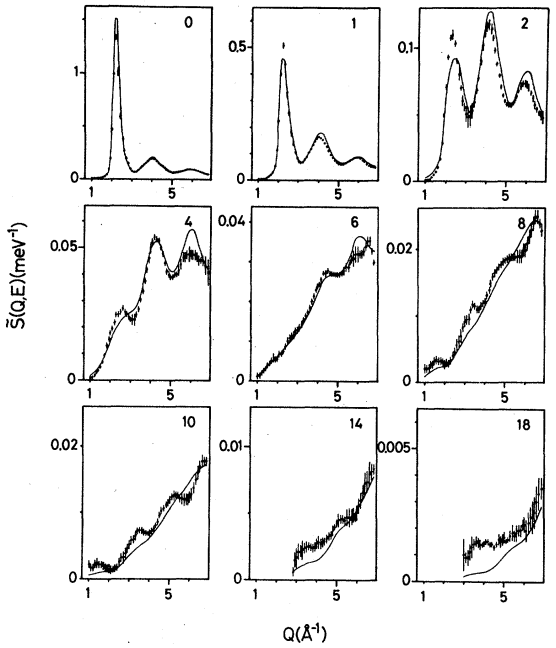

FIG. 5. The symmetrized scattering function for different energy transfers (in meV). The dots with the error bars refer to the experiments. The full line is the model, described in the Appendix, folded with the resolution in Table I.

$$E^{ig}_{max} = \hbar\left(\frac{2k_BT}{M}\right)^{1/2} Q \tag{9}$$

and is indicated in the figure. The maximum value of $E^2\tilde{S}(Q, E)$ can also be determined and is shown in Fig. 12. The corresponding value for an ideal gas is

$$\max[E^2\tilde{S}(Q, E)]^{ig} = \frac{\hbar}{e}\left(\frac{2k_BT}{\pi M}\right)^{1/2} Q \tag{10}$$

and is plotted into the figure.

The values from the model of Ailawadi, Rahman, and Zwanzig[32] were included directly in Fig. 10. The resolution according to Table II was folded to the model and the result was plotted into Figs. 3–6, 11, and 12. As can be seen from the figures this theory does not fit very well to the experimental values at small Q values. The inelastic peaks at small Q values could not be produced by the model. As Rahman[31] has pointed out, the "dispersion" curve from the spectral function $E^2\tilde{S}(Q, E)$ (Fig. 11) has nothing to do with the corresponding curve of Fig. 9.

The scattering functions presented in this paper coincide fairly well for Q values just below Q_0 and upwards to the results obtained by Randolph

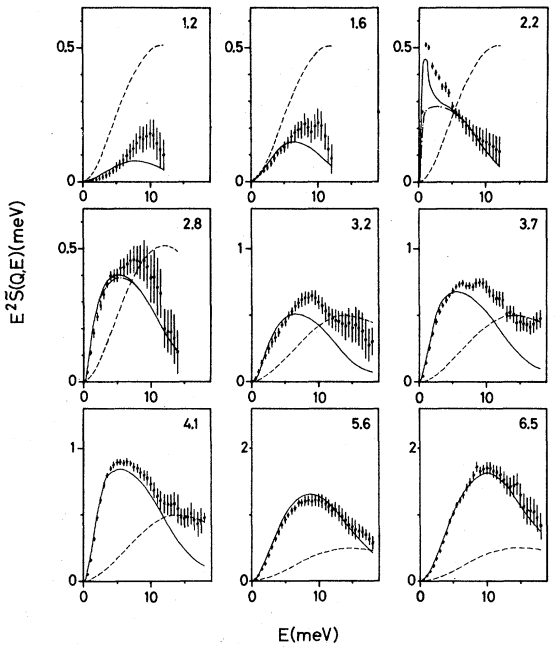

FIG. 6. The spectral function of current-current correlations for different Q values (in Å^{-1}). The notations are the same as in Fig. 3. The dash-dotted line is the model, described in the Appendix, without the resolution included.

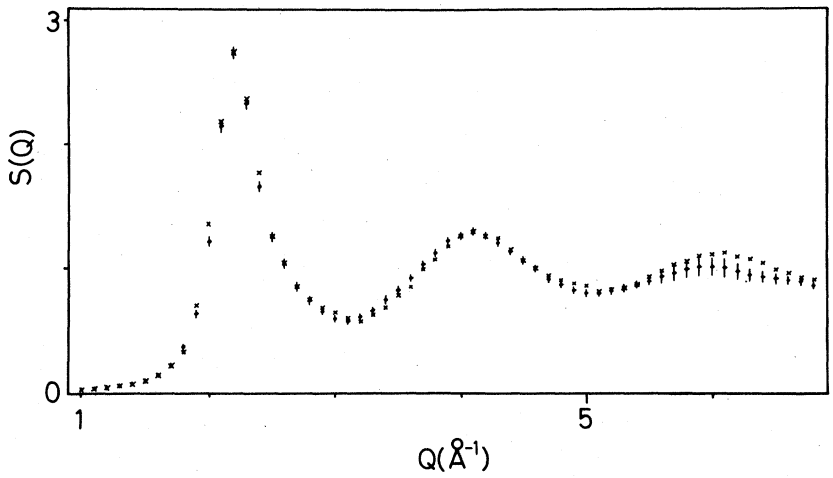

FIG. 7. The structure factor. The dots with the error bars are from the experimental scattering function integrated over E for every Q and the crosses are from an independent neutron diffraction measurement.

and Singwi[19] with the multiple-scattering correction suggested in Ref. 1, page 503 ($\gamma = 0.8$). The behavior of the spectral function $E^2\tilde{S}(Q, E)$ is very similar to the result presented by Randolph[46] including the irregular form around Q_0, which is a resolution effect (see Fig. 6).

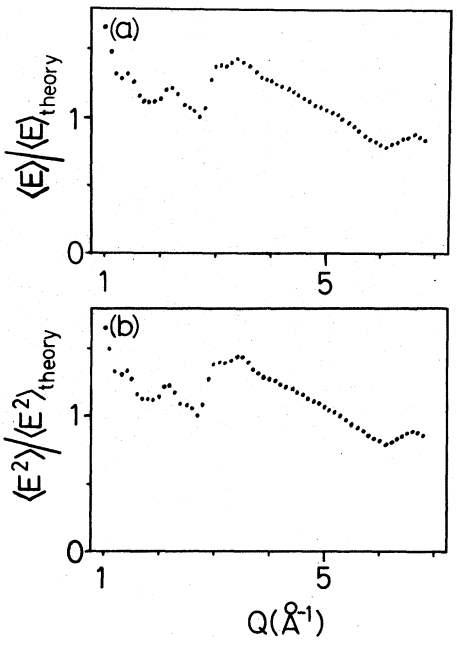

FIG. 8. (a) The first moment of the experimental scattering function compared with the exact theoretical value. (b) The second moment of the experimental scattering function compared with the exact theoretical value.

VII. CONCLUSIONS

The obtained experimental results of the symmetrized scattering function in constant Q form gave evidence for the existence of collective excitations in liquid lead. The excitations persisted up to about 60% of Q_0, which is very similar to the result obtained for liquid rubidium.[5] So it can be concluded that rubidium was not a unique exception. There are strong indications that the repulsivity of the lead potential is much higher than it is for rubidium.[7,47] Thus the existence of collective excitations in a liquid metal seems to be inde-

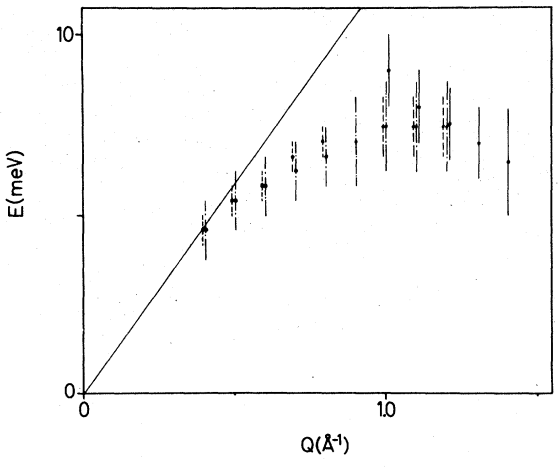

FIG. 9. The "dispersion" relation for liquid lead. The dots with full error bars are from these experiments. The dots with dashed and dash-dotted error bars have been obtained from independent experiments in a three axis crystal spectrometer. The velocity of sound is also indicated.

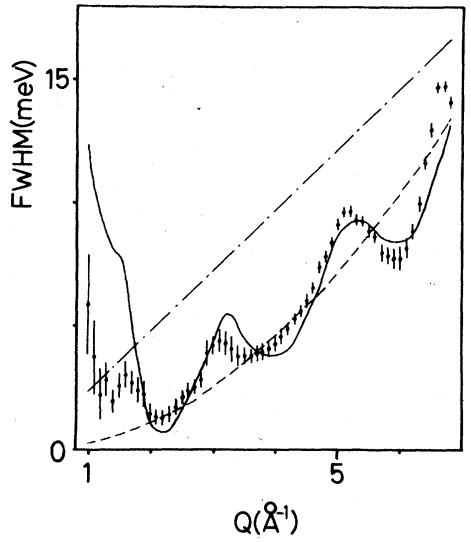

FIG. 10. FWHM of the symmetrized scattering function. The dots with the error bars are the experimental values with the resolution quadratically subtracted. The full line is the model in the Appendix, the dashed line a simple diffusion model, and the dash-dotted line an ideal gas model.

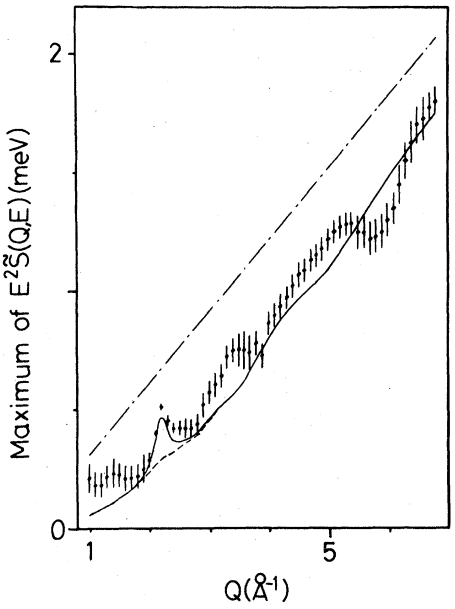

FIG. 12. The maximum value of the spectral function for current-current correlations. The notations are the same as in Fig. 11.

pendent of the softness of the core, the valence, and the electron structure. It is conceivable that the attractive part of the potential is of importance for the possibility to sustain collective excitations. This conjecture is supported by observations of the structure factors for different repulsive potentials disturbed by an attractive part.[41] Further comparisons are made in Ref. 48, where also some criteria for the existence of collective excitations in liquid metals are discussed.

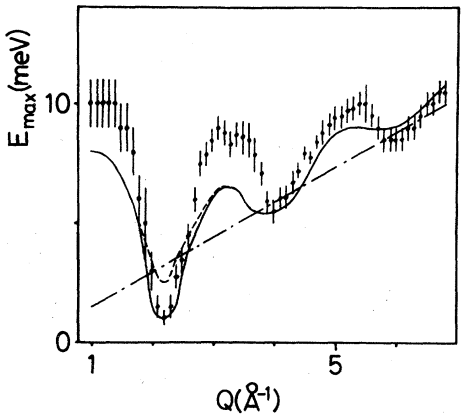

FIG. 11. Position of the peak in the spectral function of current-current correlations. The dots with the error bars come from the experiments. The full line is the model, described in the Appendix, folded with the resolution in Table I. The dashed line is the same model unfolded with the resolution. The dash-dotted line is the ideal gas model.

Mitra[7] has presented a potential for liquid lead which, however, is not based on the more recent structure factor values for small Q values.[41] Therefore, this potential is not very reliable for the long range part. This fact is probably the reason why the conclusion of Sjögren[49] for lead is contradicted by results from these measurements.

The scattering function beyond Q_0 presented here is very similar to the results obtained by Randolph and Singwi.[19] New measurements in this Q region will surely not give significantly changed values. For small Q values, however, new and better measurements would be most valuable. They should be performed in a time-of-flight spectrometer so that absolutely normalized data sets can be obtained. Proper corrections for multiple scattering are then possible to achieve. It is also desirable to minimize the multiple scattering by introducing spacers in the target,[27] but such arrangements decrease the neutron intensity on the sample. A proper theoretical analysis requires a reliable potential and shall probably be performed within the framework of kinetic theory.[50] With access to a potential also molecular dynamics studies can be made.

ACKNOWLEDGMENTS

The Swedish Natural Science Research Council has supported these experiments financially. Professor K. E. Larsson gave valuable criticism of the manuscript. Dr. M. Davidovic made some preliminary multiple-scattering calculations and also participated, together with Dr. U. Dahlborg, in the experiment, which has been published earlier and now analyzed further. Dr. L. G. Olsson gave good advice. The author thanks them all.

APPENDIX

The symmetrized scattering function in the model of Ailawadi, Rahman, and Zwanzig[32] in frequency units ($\omega = E/\hbar$) is, according to Rowe and Sköld,[51] given by

$$S(Q,\omega) = \frac{1}{\pi} \frac{\omega_0^2 \Omega^2 S(Q) K_c'(\omega)}{[\omega^2 + \omega\Omega^2 K_c''(\omega) - \omega_0^2]^2 + [\omega\Omega^2 K_c'(\omega)]^2}, \tag{A1}$$

where

$$\omega_0^2 = \frac{k_B T Q^2}{M S(Q)}, \tag{A2}$$

$$\Omega^2 = \frac{M\langle\omega^4\rangle}{k_B T Q^2} - \omega_0^2, \tag{A3}$$

$$K_c'(\omega) = \frac{\tau\sqrt{\pi}}{2} e^{-\omega^2\tau^2/4}, \tag{A4}$$

$$K_c''(\omega) = -\tau D(\omega\tau/2), \tag{A5}$$

D is the Dawson integral and, according to Rahman (from Ref. 51),

$$\tau = 1/\Omega. \tag{A6}$$

The fourth moment in (A3) is approximately given by

$$\langle\omega^4\rangle = \omega_0^2\left[\frac{3Q^2 k_B T}{M} + \omega_E^2\left(1 - \frac{3\sin QR_0}{QR_0} - \frac{6\cos QR_0}{(QR_0)^2} + \frac{6\sin QR_0}{(QR_0)^3}\right)\right]. \tag{A7}$$

The quantity ω_E has been chosen to the maximum frequency that is seen in the dispersion relation for liquid lead[27] and R_0 is where the pair distribution function has its first maximum.[40]

[1] J. R. D. Copley and S. W. Lovesey, Rep. Prog. Phys. 38, 461 (1975).
[2] S. W. Lovesey and J. R. D. Copley, *Neutron Inelastic Scattering 1977* (IAEA, Vienna, 1978), Vol. II, p. 3.
[3] K. Sköld, J. M. Rowe, G. Ostrowski, and P. D. Randolph, Phys. Rev. A 6, 1107 (1972).
[4] H. G. Bell, H. Moeller-Wenghoffer, A. Kollmar, R. Stockmeyer, T. Springer, and H. Stiller, Phys. Rev. A 11, 316 (1975).
[5] J. R. D. Copley and J. M. Rowe, Phys. Rev. Lett. 32, 49 (1974); Phys. Rev. A 9, 1656 (1974).
[6] S. K. Mitra and M. J. Gillan, J. Phys. C 9, L515 (1976).
[7] S. K. Mitra, J. Phys. C 11, 3551 (1978).
[8] U. Dahlborg and I. Ebbsjö (private communication).
[9] I. Ebbsjö, T. Kinell, and I. Waller, J. Phys. C 11, L50 (1978); J. Phys. C 13, 1865 (1980).
[10] L. Koester, *Springer Tracts in Modern Physics, Neutron Physics* (Springer, Berlin, 1977), Vol. 80, p. 1.
[11] R. B. Gordon, Acta Metall. 7, 1 (1959).
[12] P. A. Egelstaff, Acta Crystallogr. 7, 673 (1954).
[13] B. N. Brockhouse, Phys. Rev. 98, 1171 (1955).
[14] B. N. Brockhouse and N. K. Pope, Phys. Rev. Lett. 3, 259 (1959).
[15] I. Pelah, W. L. Whittemore, and A. W. McReynolds, Phys. Rev. 113, 767 (1959).
[16] H. Palevsky, *Inelastic Scattering of Neutrons in Solids and Liquids* (IAEA, Vienna, 1961), p. 265.
[17] K. C. Turberfield, Proc. Phys. Soc. London 80, 395 (1962).
[18] M. J. Cotter, Ph.D. thesis, Fordham University, University Microfilms, Ann Arbor Michigan, Report No. 63-201, 1962 (unpublished).
[19] P. D. Randolph and K. S. Singwi, Phys. Rev. 152, 99 (1966).
[20] S. J. Cocking and P. A. Egelstaff, Phys. Lett. 16, 130 (1965).
[21] S. J. Cocking and P. A. Egelstaff, J. Phys. C 1, 507 (1968).
[22] S. J. Cocking, Adv. Phys. 16, 189 (1967).
[23] S. J. Cocking, United Kingdom Atomic Energy Authority Report No. AERE-R 5867, 1968 (unpublished).
[24] G. D. Wignall and P. A. Egelstaff, J. Phys. C 1, 519 (1968).
[25] B. Dorner, T. Plesser, and H. Stiller, Physica (The Hague) 31, 1537 (1965); Discuss. Faraday Soc. 43, 160 (1967).
[26] O. Söderström, M. Davidovic, U. Dahlborg, and K. E. Larsson, *Neutron Inelastic Scattering 1977* (IAEA, Vienna, 1978), Vol. II, p. 67.
[27] O. Söderström, J. R. D. Copley, J.-B. Suck, and B. Dorner, J. Phys. F 10, L151 (1980).
[28] G. L. Squires, *Introduction to the Theory of Thermal Neutron Scattering* (Cambridge University Press, Cambridge, 1978).
[29] W. Marshall and S. W. Lovesey, *Theory of Thermal Neutron Scattering* (Oxford University Press, Oxford, 1971).
[30] P. Schofield, Phys. Rev. Lett. 4, 239 (1960).
[31] A. Rahman, Phys. Rev. Lett. 19, 420 (1967).
[32] N. K. Ailawadi, A. Rahman, and R. Zwanzig, Phys. Rev. A 4, 1616 (1971).
[33] L. G. Olsson, U. Dahlborg, M. Grönros, L. E. Karlsson, K. E. Larsson, and T. Månsson, Nucl. Instrum. Methods 123, 99 (1975).
[34] L. G. Olsson (private communication).
[35] J. R. D. Copley, D. L. Price, and J. M. Rowe, Nucl.

Instrum. Methods 107, 501 (1973); 114, 411 (1974).
[36]O. Söderström, thesis at the The Royal Institute of Technology in Stockholm, 1980 (unpublished).
[37]S. J. Cocking and C. R. T. Heard, Atomic Energy Research Establishment Report No. AERE-R 5016, HMSO, London, 1965 (unpublished).
[38]J. R. D. Copley, Comput. Phys. Commun. 7, 289 (1974); 9, 59 (1975).
[39]J. R. D. Copley (private communication).
[40]U. Dahlborg, M. Davidovic, and K. E. Larsson, Phys. Chem. Liq. 6, 149 (1977).
[41]U. Dahlborg and L. G. Olsson, Proceedings of the LAM4 Conference in Grenoble, 1980 (in press).
[42]Subroutines VCO3A and TGO1A in Harwell Subroutine Library, Atomic Energy Research Establishment Report No. AERE-R 7477 (compiled by M. J. Hopper), 1973 (unpublished).
[43]M. W. Johnson, B. McCoy, N. H. March, and D. J. Page, Phys. Chem. Liq. 6, 243 (1977).
[44]A complete table is available from the author.
[45]T. E. Faber, *An Introduction to the Theory of Liquid Metals* (Cambridge University Press, Cambridge, 1972).
[46]P. D. Randolph, Phys. Rev. Lett. 20, 531 (1968).
[47]R. Evans, *Microscopic Structure and Dynamics of Liquids*, NATO Advanced Study Institute, edited by J. Dupuy and A. J. Dianoux (Plenum, New York, 1978).
[48]O. Söderström, J. R. D. Copley, J.-B. Suck, and B. Dorner, Proceedings of the LAM4 Conference in Grenoble, 1980 (in press).
[49]L. Sjögren, J. Phys. C 12, 425 (1979).
[50]L. Sjögren and A. Sjölander, Ann. Phys. (N.Y.) 110, 122 (1978); J. Phys. C 12, 4369 (1979).
[51]J. M. Rowe and K. Sköld, *Neutron Inelastic Scattering 1972* (IAEA, Vienna, 1972), p. 413 (with corrigendum).